A Bayesian method for pulse shape and energy estimation for gamma spectrometry measurements using semiconductor detectors

G. Montémont*, M. Arquès* and A. Mohammad-Djafari†

*LETI-CEA Technologies Avancées
CEA Grenoble, 17 rue des Martyrs, F38054 Grenoble cedex 9, France
†Laboratoire Signaux et Systèmes, Supélec, Plateau de Moulon
3 rue Joliot-Curie, F91192 Gif-sur-Yvette cedex, France

Abstract. The gamma spectroscopy principle is to evaluate a gamma ray energy by measuring the quantity of free charges generated by the gamma-ray absorption. Semiconductors like CdTe and CdZnTe are promising materials for this application. However, they encounter a major drawback: due to imperfections in their charge transport properties, the transient signal induced by a gamma ray has a varying shape. This phenomenon severely degrades energy resolution. The measured pulse amplitude depends not only on the gamma-ray energy but also on the interaction location. The aim of this paper is to present a new approach based on the Bayesian probabilistic inference, to estimate jointly the pulse shape and the energy. It brings a methodology for founding a relevant estimation of gamma-ray energy associated with a pulse. The pulse shape variability is modeled by assigning a prior probability law on his dispersion around its nominal shape. Then, using this prior knowledge and the observations, we tried to estimate jointly the pulse shape and its amplitude that correspond to the associated energy of the gamma-ray energy.

INTRODUCTION

The aim of gamma-ray spectroscopy is to determine which energies constitute an incident gamma radiation. Application domains are nuclear industry, medical imagery and scientific instrumentation.

One way of detecting gamma-rays is to use semiconductor detectors. The incident radiation generates in the semiconductor bulk electron-hole pairs. The number of generated charge carriers is proportional to the interacting gamma-ray energy and the charge is collected by applying an electric field between two electrodes deposed on the semiconductor. Thus, one can measure a transient pulse associated to the gamma-ray interaction.

CdZnTe is a leading material for room-temperature gamma-ray spectroscopy. Its physical properties, such as high atomic number, high room-temperature resistivity and good electron transport properties are well-suited for this application. However, though recents technological improvements, CdZnTe still has some drawbacks. Hole transport properties are very poor and material bulk is not uniform. As a consequence of these physical defects, the obtained pulse shape is not constant. It depends on gamma-ray interaction location in the detector. In addition of this pulse shape uncertainty, the pulse signal is altered by an electronic noise. To compensate for the degradation induced by pulse shape uncertainty, two types of methods have been used: electrode design and

electronic corrections.

The Frisch grid effect, obtained by modifying electrode design, allows a huge reduction of pulse shape variations [1] but the technological process is complex and expensive. Electronic correction techniques [2] are cheaper. They are based on pulse shape analysis techniques, with the aim of compensating for the effect of shape variations on energy estimation.

As the main physical source of pulse shape variation is the carrier transit time, many pulse processing techniques rely on this information and use a pulse duration estimator [3, 5]. These methods are based on a simple but relevant prior knowledge and are quite efficients. Some refined methods use a parametrical pulse shape model prior [7, 8]. The main difficulty is then to find an accurate model of the pulse shape because physical behaviour of the detector is very complex. Neural networks have also been tested [6]. Their learning capabilities allow adaptation of the processing scheme to the real pulse shape evolutions.

The main difficulty in our application is avoiding count rate limitation, so that we cannot use numerical iterative methods. We have to use direct estimators and to implement them with an analog circuit. Some approximations allow this direct estimation. The experimental results show that even this suboptimal approximate solution brings good performances. We have developed a new correction technique using Bayesian probalistic inference to estimate jointly the pulse shape and the energy. Our prior knowledge is then a probabilistic model.

In the first part, we present the state of the art in terms of pulse processing methods for semiconductor detectors and we compare the different approaches. In the second part, the Bayesian framework is introduced. In the third part, we propose to use an appropriate entropic prior law for the pulse shape and we discuss its suitability to detector's physical behaviour and apply Bayesian methodology to it. Finally, in a fourth part, we show some results on real data and comment on them.

BAYESIAN ESTIMATION

The structure of our observation model is very simple:

$$X(t) = ES(t) + B(t)\,, \tag{1}$$

where E is the gamma-ray energy, $S(t)$ the signal shape and $B(t)$ the electronic noise.

To simplify the notation, we use a vector representation of signals:

$$\mathbf{X} = E\mathbf{S} + \mathbf{B} \quad \text{or} \quad X_i = ES_i + B_i \quad \text{with } i = 1 \cdots n\,, \tag{2}$$

where $\mathbf{X}$, $\mathbf{S}$ and $\mathbf{B}$ are, respectively, vectors containing the samples (X_i, S_i and B_i) of the observed signal, the pulse shape and the noise.

Joint posterior probability law

For estimating the energy E and the shape $\mathbf{S}$, we maximize the joint posterior law,

$$P(E,\mathbf{S}|\,\mathbf{X}) \propto P(\mathbf{X}|\,E,\mathbf{S})P(\mathbf{S})P(E)\,. \tag{3}$$

For spectrometric applications, we use a uniform prior law on E, e.g. $P(E) = 1/E_{\max}$ on the interval $[0,E_{\max}]$. Electronic noise is assumed to be additive, centered and Gaussian. Thus we have

$$P(\mathbf{X}|\,E,\mathbf{S}) \propto \exp\left\{-\frac{1}{2}(\mathbf{X}-E\mathbf{S})^t\Gamma_{\mathbf{B}}^{-1}(\mathbf{X}-E\mathbf{S})\right\}\,, \tag{4}$$

where $\Gamma_{\mathbf{B}}$ is the noise covariance matrix. To account for the variability of the pulse shape around its nominal shape $\mathbf{S}_0$, we assign a prior probability law:

$$P(\mathbf{S}) \propto \prod_j \exp\left\{-\sum_j g(S_j,S_{0_j})\right\}\,, \tag{5}$$

where g is a function which increases when S_j go farther from S_{0_j}.

Then, the joint probability of having an energy E and a shape $\mathbf{S}$ with an observation $\mathbf{X}$ is

$$P(E,\mathbf{S}|\,\mathbf{X}) \propto \exp\left\{-\frac{1}{2}(\mathbf{X}-E\mathbf{S})^t\Gamma_{\mathbf{B}}^{-1}(\mathbf{X}-E\mathbf{S})\right\}\cdot\exp\left\{-\sum_j g(S_j,S_{0_j})\right\}\,, \tag{6}$$

and the associated potential function is:

$$F = -\ln P(E,\mathbf{S}|\,\mathbf{X}) = \frac{1}{2}(\mathbf{X}-E\mathbf{S})^t\Gamma_{\mathbf{B}}^{-1}(\mathbf{X}-E\mathbf{S}) + \sum_j g(S_j,S_{0_j}). \tag{7}$$

Maximizing the posterior law $P(E,\mathbf{S}|\,\mathbf{X})$ is equivalent to minimizing the potential function F.

Joint MAP estimation system

The minimum of F is found by the system:

$$\begin{cases} \dfrac{\partial F}{\partial E} = 0 \\ \nabla_{\mathbf{S}} F = \mathbf{0}\,, \end{cases} \tag{8}$$

and if $\widehat{E}$ and $\widehat{\mathbf{S}}$ are the optimal estimators of the energy and the shape, we obtain

$$\begin{cases} -\widehat{\mathbf{S}}^t\Gamma_{\mathbf{B}}^{-1}(\mathbf{X}-\widehat{E}\widehat{\mathbf{S}}) = 0 \\ -\widehat{E}\Gamma_{\mathbf{B}}^{-1}(\mathbf{X}-\widehat{E}\widehat{\mathbf{S}}) + \mathbf{g}'(\widehat{\mathbf{S}},\mathbf{S}_0) = \mathbf{0}\,, \end{cases} \tag{9}$$

where $\mathbf{g}' = \left[\frac{\partial g}{\partial S_1},\cdots,\frac{\partial g}{\partial S_n}\right]$.

Solution

The exact solution of the system should be found iteratively. For avoiding count rate limitation in online processing and for reducing processing time, we tried to obtain an approximate but direct solution and implemented the resulting algorithm via an analog circuit design.

Our approximation is based on a low-noise hypothesis: a first order estimation of $\widehat{E}\widehat{\mathbf{S}}$ is given by the observation $\mathbf{X}$. With this initial guess, we realize one iteration step of the gradient algorithm:

$$\widehat{\mathbf{S}} \simeq \frac{\mathbf{X}}{\widehat{E}} - k\nabla_{\mathbf{S}} F_{\{\mathbf{S}=\mathbf{X}/\widehat{E}\}} = \frac{\mathbf{X}}{\widehat{E}} - k\mathbf{g}'(\frac{\mathbf{X}}{\widehat{E}}, \mathbf{S}_0) \ , \tag{10}$$

where k is a scalar coefficient. Replacing it in the equation $\frac{\partial F}{\partial E} = 0$, we have

$$\mathbf{X}^t \Gamma_{\mathbf{B}}^{-1} \mathbf{g}'(\frac{\mathbf{X}}{\widehat{E}}, \mathbf{S}_0) = 0 \ . \tag{11}$$

GAUSSIAN PRIOR EXAMPLE

As a first example, we consider the case where $g(S_j, S_{0_j}) = 1/2(S_j - S_{0_j})^2$ which assumes that pulse shapes are distributed symetrically around the nominal shape $\mathbf{S}_0$. To simplify the equations we assume also that the noise is uncorrelated ($\Gamma_{\mathbf{B}} = Id$). Then the Eqs. (10) and (11) become

$$\begin{cases} \widehat{\mathbf{S}} = \dfrac{\mathbf{X}}{E} - k\left(\dfrac{\mathbf{X}}{E} - \mathbf{S}_0\right) = (1-k)\dfrac{\mathbf{X}}{E} + k\mathbf{S}_0 \\ \mathbf{X}^t\left(\dfrac{\mathbf{X}}{E} - \mathbf{S}_0\right) \rightarrow \widehat{E} = \dfrac{\mathbf{X}^t\mathbf{X}}{\mathbf{X}^t\mathbf{S}_0} \ . \end{cases} \tag{12}$$

The first equation shows that the best estimate of the shape is a linear combination of data ($\mathbf{X}/E$) and the a priori solution $\mathbf{S}_0$. The best estimate of the energy $\widehat{E}$ is obtained from the second equation. If we note by $M_1(t) = \int X(t)X(t-\tau)\,d\tau$ and by $M_2(t) = \int X(t)S_0(t-\tau)\,d\tau$, we can imagine an electronic circuit to obtain $M_1(t)$ and $M_2(t)$ from which we can deduce the energy $\widehat{E}$ (Fig. (1)).

In the next section we discuss the appropriate expression of $g(S_j, S_{0_j})$ for our application.

ENTROPIC PRIOR LAW

Level distribution

In CdZnTe detectors, hole transport properties are very poor and only electron-induced signal can be observed. Because of the difference of transit length and electron

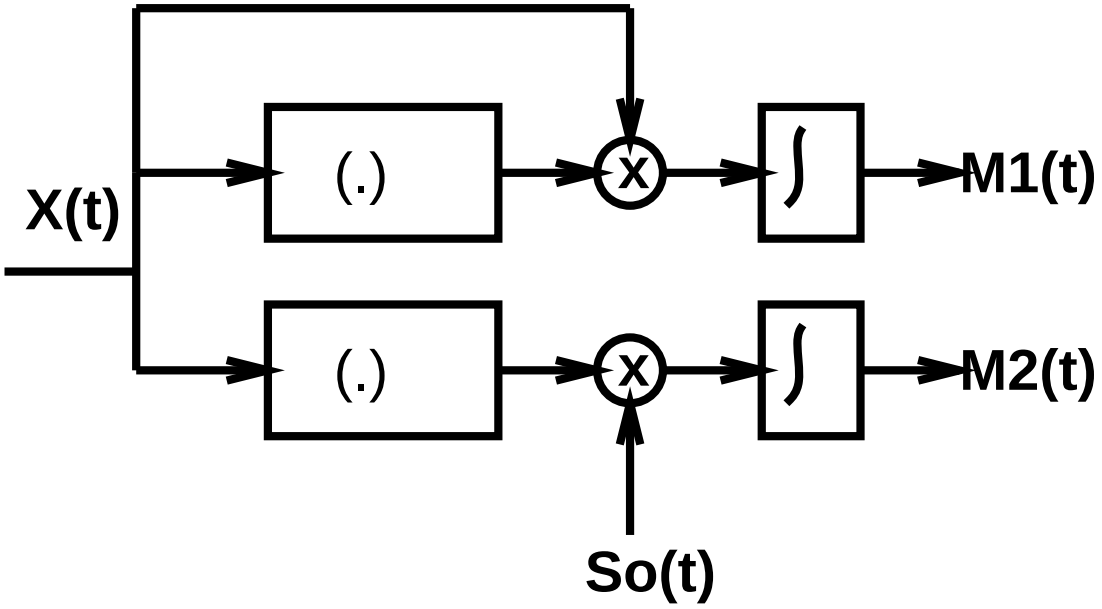

FIGURE 1. The Gaussian estimator implementation (with uncorrelated noise). Observation data $X(t)$ are not modified before the correlator stage.

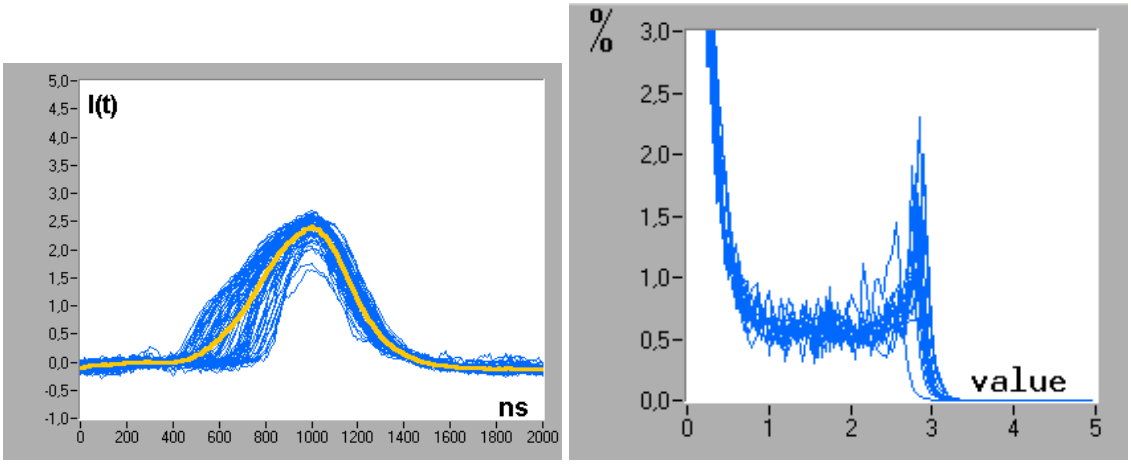

FIGURE 2. (left) sampled current pulse shapes from a CdZnTe detector generated by 122 keV photons compared to the mean pulse shape (thick line). (right) superposition of pulse histograms.

trajectories, this signal shape is not constant. Figure (2) shows some pulse shapes that occur with a 122 keV-photon interaction. We can observe that there is a maximum current value and that current level distribution has a peak at this value. This maximum current corresponds to the motion of the totality of generated electrons in the detector electric field. We cannot have more moving electrons than the number generated by the gamma-ray, therefore current value cannot excess this level. This kind of distribution

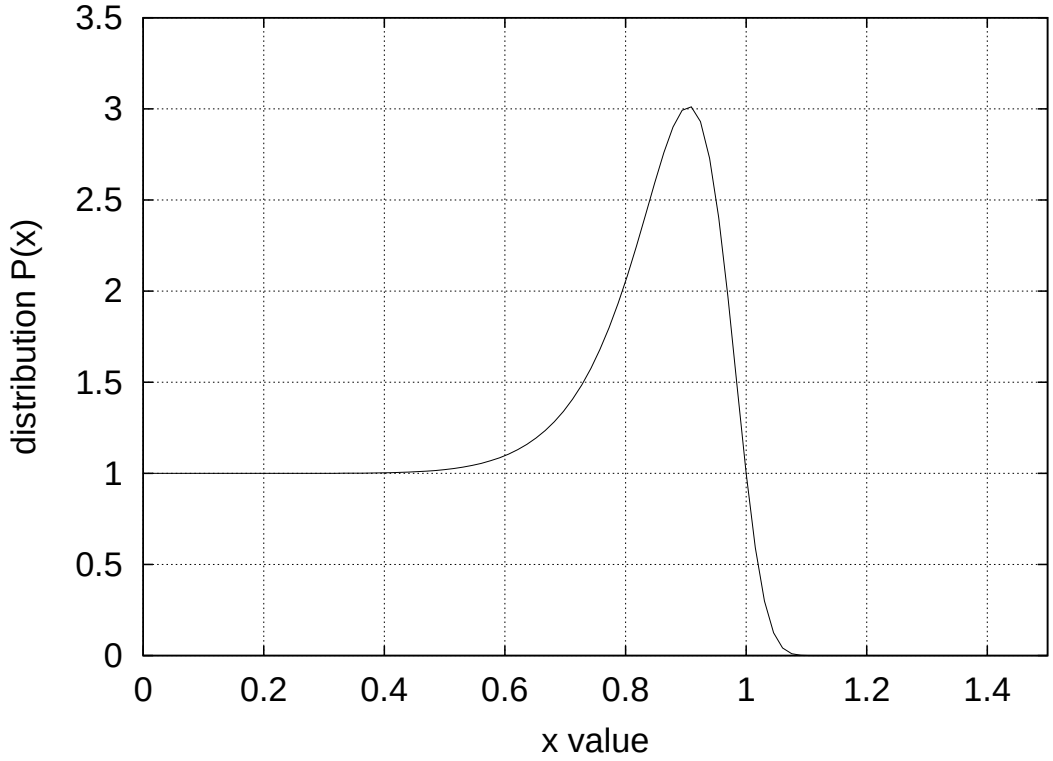

FIGURE 3. An entropic distribution law: function $\exp\{-30.x^{10}.\ln x\}$.

can be modeled by an entropic law (as seen in Fig. (3)):

$$P(S_j) = \exp\left\{-\lambda S_j^{\alpha} \ln \frac{S_j}{S_{0_j}}\right\} . \tag{13}$$

The potential function associated with the entropic law is

$$g(S_j) = \lambda S_j^{\alpha} \ln \frac{S_j}{S_{0_j}} \longrightarrow g'(S_j) = \lambda S_j^{\alpha-1}(1+\alpha \ln \frac{S_j}{S_{0_j}}) . \tag{14}$$

Energy estimator

Replacing $\mathbf{g}'(\mathbf{X}/\widehat{E})$ in Eq. (11), we have:

$$\mathbf{X}^t \Gamma_{\mathbf{B}}^{-1} \left(\mathbf{X}^{\alpha-1} \cdot\star (\mathbf{1} + \alpha \ln \mathbf{X} - \alpha \ln E \mathbf{S}_0)\right) = 0 , \tag{15}$$

where we used the Matlab notation $(\cdot\star)$ to mean pointwise multiplication of two vectors: $\mathbf{X} \cdot\star \mathbf{Y} = \mathbf{Z}$ with $z_i = x_i y_i$. The energy estimator is:

$$\widehat{E} \propto \exp\left\{\frac{\mathbf{X}^t \Gamma_{\mathbf{B}}^{-1} (\mathbf{X}^{\alpha-1} \cdot\star (\ln \mathbf{X} - \ln \mathbf{S}_0)}{\mathbf{X}^t \Gamma_{\mathbf{B}}^{-1} \mathbf{X}^{\alpha-1}}\right\} . \tag{16}$$

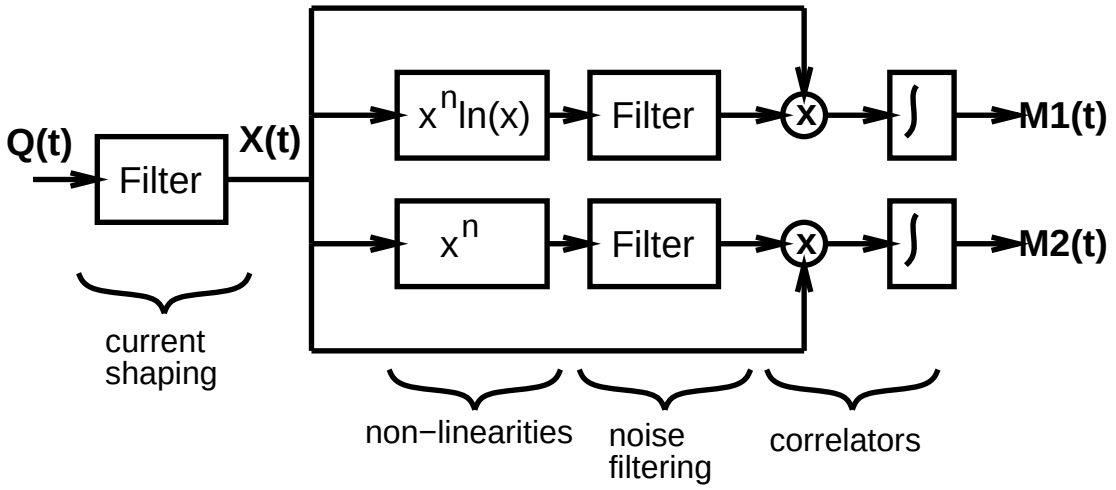

FIGURE 4. The entropic estimator implementation.

The coefficient α tunes the sharpness of level distribution. One can observe that with high α, only the higher values of the pulse are used for energy estimation.

Implementation

The implementation scheme is described on Fig. (4). In this scheme, $S_0(t)$ is assumed to be constant and equal to the current induced by electron motion due to electric field (typically, this current is 0.1 nA/keV). We use two processing channel. On the first one is computed

$$M_1 = \max M_1(t) = \mathbf{X}^t \Gamma_{\mathbf{B}}^{-1} (\mathbf{X}^{\alpha-1} \cdot\star \ln \mathbf{X}) \,, \tag{17}$$

$M_1(t)$ being the correlation signal between $X(t)$ and $\Gamma_{\mathbf{B}}^{-1} * X(t)^{\alpha-1} \ln X(t)$. On the second one is computed

$$M_2 = \max M_2(t) = \mathbf{X}^t \Gamma_{\mathbf{B}}^{-1} \mathbf{X}^{\alpha-1} \,, \tag{18}$$

$M_2(t)$ being the correlation signal between $X(t)$ and $\Gamma_{\mathbf{B}}^{-1} * X(t)^{\alpha-1}$.

At the preamplifier output, the pulses are integrated because we use a charge-sensitive amplifier. A first stage perform a derivation for producing current-shaped pulses $X(t)$. We have to apply two non-linearities ($x^n \ln x$ and x^n, with $n = \alpha - 1$) on two different channels. A typical value is $n = 3$ or $= 4$. Transformed pulses are filtered by $\Gamma_{\mathbf{B}}^{-1}$ for compensating noise and outputs are correlated with $X(t)$. In our case, this filtering is a low-pass filter. Its cut-off frequency (typically 200 kHz) depends on noise spectrum. We measure the maxima M_1 and M_2 of the two correlation signals and apply the division and exponentiation from Eq. (16): $\widehat{E} \propto \exp(M_1/M_2)$.

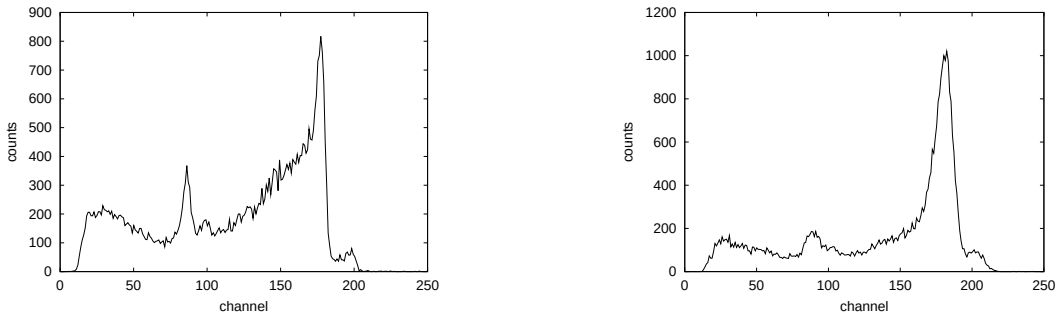

(a) 500 ns shaping time (b) 100 ns shaping time

FIGURE 5. Spectra obtained by linear processing. For reducing the peak-tailing effect due to charge loss, a high frequency filtering is needed. Band-pass filters have first order cut-offs.

EXPERIMENTAL RESULTS

Experimental setup

The processing scheme was applied to 6 mm thick HPBM-grown CdZnTe detectors. They were irradiated with a ^{57}Co source, with a main energy peak at 122 keV.

Detectors electrode geometry is planar and charge are drifted with a 500 V bias voltage. Then, electron transit time is typically 500 ns. We used a eV-5093 charge-sensitive preamplifier from EV-PRODUCTS. Though our processing system is designed for analog implementation, the validation experiments were done on sampled signals. Pulses were digitalized by a DA500A SIGNATEC acquisition board featuring an analog to digital converter. Our sampling rate was 100 MHz with a 8-bit coding. The processing task relied on a computer. A standard linear shaping was implemented beside of the non-linear processing scheme.

Linear filtering

As a comparison, we have implemented a classical linear processing scheme. After sampling, the pulse is filtered by a band pass filter. Then, the maximum value of filtered signal is taken as measurement.

This linear method, based on gaussian optimal filtering framework, is only convenient if pulse shape is constant. Because of pulse shape variations, this method encounters some limitations in our case.

With low frequency band-pass filtering (shaping time longer than transit time), the system measures the collected charge. In our case, because of hole trapping in the material bulk, there is a charge collection loss, and we obtain a tailed peak.

With high frequency band-pass filtering (shaping time short beside electron transit time), the system measures rather the maximum current. This current is almost constant in all case and there is no peak tailing but the measurement is strongly degraded by noise. Even long pulses are shaped with short times, and there is an information loss.

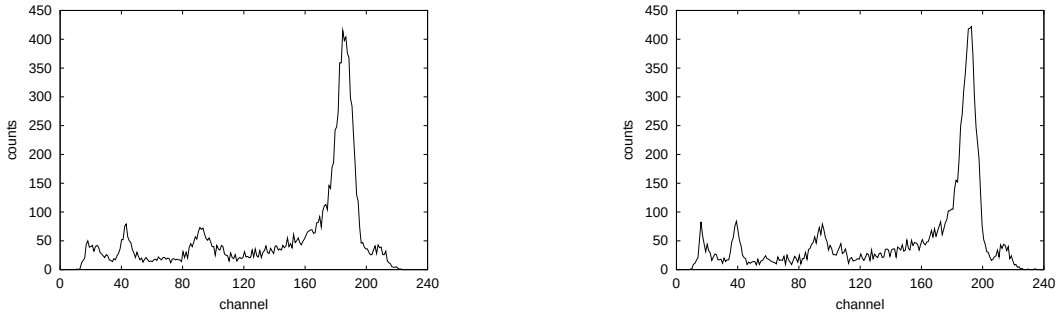

(a) linear shaper (b) entropic estimator ($\alpha = 4$)

FIGURE 6. Spectra obtained by linear and entropic processing with the same sampled pulse set. Energy resolution for the main peak (122 keV) are 7.1% FWHM for linear shaper and 6.2% FWHM for entropic estimator.

The goal of our approach is to solve this problem by adapting the shaping to the observed pulse shape by using a non-linearity.

Entropic estimator

We have compared the performances of the entropic estimator with those obtained by linear shaping by applying both methods on the same sampled pulses. Both spectra show the same energy peaks: the main 122 keV peak, a little 136 keV peak and some fluorescence escape peaks at lower energies ($\sim$ 60 keV). Energy resolutions (given by the full-width at half maximum or FWHM) at 122 keV are in general 1% better with the entropic estimator than with the linear shaper (Fig. (6)). This resolution improvement is significant beside the optimal resolution value (about 5%, see Fig. (7)). The peak is a little sharper and the separation between 122 and 136 keV peaks is more obvious.

However, performance increase is limited by two factors:

- the detector behaviour is complex and an accurate model is very difficult to find because each detector needs its own model;
- with the described detection system, even with an optimal processing scheme, simulation has proven that shape variations limit resolution to $\sim$ 5%.

For solving the first problem, one solution is the bi-parametric approach: both correlation measurements M_1 and M_2 (Fig. (4)) are stocked in computer memory. Energy estimation is done with an offline calibration (different for each detector): the estimator formula $\exp(M_1/M_2)$ is replaced by a relation deduced from detector experimental data $\widehat{E} = f(M_1, M_2)$ (Fig. (8)). With this method, we can reach a 5.0% energy resolution. The second problem is not in the field of signal processing, but there are physical or electronical solutions: working on material elaboration, electrode design and preamplifier optimization.

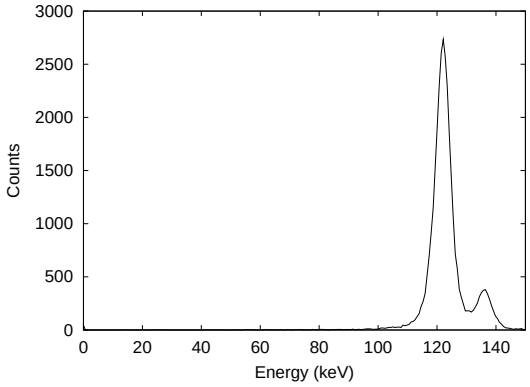

FIGURE 7. 6 mm thick detector CdZnTe: simulated 122 and 136 keV spectrum, with an optimal energy estimation (the same parametrical pulse model was used for simulation and estimation). Energy resolution is 4.7% FWHM.

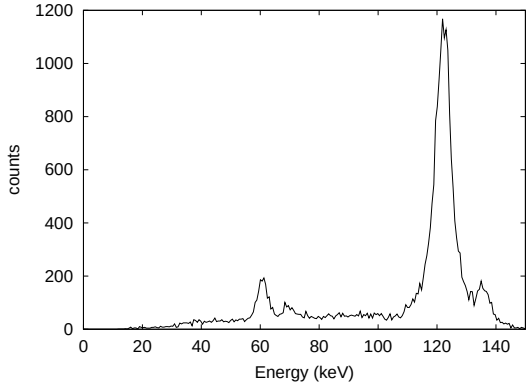

FIGURE 8. 6 mm thick detector CdZnTe: spectrum obtained with entropic estimator ($\alpha = 4$) with offline calibration. Energy resolution is 5.0% FWHM and there is no peak tailing.

CONCLUSION

We have presented a Bayesian approach for estimating gamma-ray energy with CdZnTe semiconductor detectors. This framework allows one to take account for some shape prior knowledge. Results show the efficiency of this method but also its limits. Offline calibration is needed for adapting the estimation to each detector and improvements in detection system design can also lead to significant advances.

REFERENCES

1. P.N. Luke, (1996) Electrode configuration and energy resolution in gamma-ray detectors, *Nucl. Inst. Meth.*, **A380**, pp. 232–237.
2. M. Richter & P. Siffert, (1992) High resolution gamma ray spectroscopy with CdTe detector systems, *Nucl. Inst. Meth.*, **A322**, pp. 529-537.

3. Hess *et al.*, (1994) Analysis of the pulse shapes obtained from single crystal $Cd_{0.9}Zn_{0.1}Te$ radiation detectors, *Nucl. Inst. Meth.*, **A353**, pp. 76–79.
4. J.C. Lund *et al.*, (1996) The use of pulse processing techniques to improve the performance of CdZnTe gamma-ray spectrometers, *IEEE Trans. Nucl. Sci.*, **43(3)**.
5. L. Verger *et. al.*, (1997) New developments of CdTe and CdZnTe detectors for X and γ-ray applications, *J. Elec. Mat.*, **26(6)**, pp. 738–744.
6. Y. Takenaka *et al.*, (1996) Energy resolution enhancement of CdTe semiconductor detector spectra by using a neural network algorithm, *Nucl. Inst. Meth.*, **A369**, pp. 637–641.
7. H. Takahashi *et al.*, (1996) Signal processing for CdTe detectors using a fast signal digitizing technique, *Nucl. Inst. Meth.*, **A380**, pp. 381–381.
8. Ch. Bargholtz *et al.*, (1999) Model-based pulse shape correction for CdTe detectors, *Nucl. Inst. Meth.*, **A434**, pp. 399–411.